OncoTargets and Therapy

Dovepress
open access to scientific and medical research

Open Access Full Text Article

ORIGINAL RESEARCH

Bioactive Compounds from *Abelmoschus manihot L.* Alleviate the Progression of Multiple Myeloma in Mouse Model and Improve Bone Marrow Microenvironment

This article was published in the following Dove Press journal:
OncoTargets and Therapy

Jianhao Hou,[1,2,*] Jinjun Qian,[2,*] Zhenlin Li,[3,4,*] Aixiu Gong,[5] Sixia Zhong,[2] Li Qiao,[2] Shihui Qian,[3,4] Yanxin Zhang,[2] Renjie Dou,[2] Rui Li,[2] Ye Yang,[2] Chunyan Gu[1,2]

[1]The Third Affiliated Hospital of Nanjing University of Chinese Medicine, Nanjing 210001, People's Republic of China; [2]School of Medicine and Holistic Integrative Medicine, Nanjing University of Chinese Medicine, Nanjing 210023, People's Republic of China; [3]Jiangsu Province Academy of Traditional Chinese Medicine, Nanjing 210028, People's Republic of China; [4]Jiangsu Provincial Platform for Conservation and Utilization of Agricultural Germplasm, Nanjing 210028, People's Republic of China; [5]Department of Stomatology, Children's Hospital of Nanjing Medical University, Nanjing 210009, People's Republic of China

*These authors contributed equally to this work

Correspondence: Ye Yang
School of Medicine and Holistic Integrative Medicine, Nanjing University of Chinese Medicine, Nanjing 210023, People's Republic of China
Tel +86 25 8581 1597
Email yangye876@sina.com

Shihui Qian
Jiangsu Province Academy of Traditional Chinese Medicine, Shizi Street Hongshan Road, Nanjing 210028, People's Republic of China
Email njqsh2005@126.com

Purpose: *Abelmoschus manihot* (L.) Medik. (Malvaceae) derived Huangkui capsules (HKC) represent a traditional Chinese medicine that has been widely applied to the clinical therapy of kidney and inflammatory diseases. The present study aimed to determine the potential therapeutic effects and underlying mechanisms of the ingredients on Multiple Myeloma (MM), an incurable disease that exhibits malignant plasma cell clonal expansion in the bone marrow.

Methods: A 5TMM3VT syngeneic MM-prone model was established and treated with HKC. Murine pre-osteoblast MC3T3-E1 and pre-osteoclast Raw264.7 cells were treated with nine flavonoid compounds extracted from the flowers of *Abelmoschus manihot*. MC3T3-E1 and Raw264.7 cells were then examined by alizarin red staining and tartrate-resistant acid phosphatase activity staining, respectively. The proliferation of two human MM cells (ARP1, H929) was examined by performing an MTT assay following treatment with flavonoid compounds. Additionally, the cell cycle was analyzed via staining and flow cytometry. The differential expressions of certain proteins were detected via Western blotting, transcriptomic RNA-sequencing as well as RT-qPCR.

Results: The results revealed that MM-prone animals appeared to be protected following HKC treatment, as evidenced by a prolonged survival rate. Furthermore, four of the nine flavonoid compounds [Hyperin/Hyperoside, HK-2; Cannabiscitrin, HK-3; 3-*O*-kaempferol-3-*O*-acetyl-6-*O*-(p-coumaroyl)-β-D-glucopyranoside, HK-11; 8-(2''-pyrrolidione-5''-yl)-quercetin, HK-B10] induced the differentiation of murine pre-osteoblast MC3T3-E1 cells. In addition, two compounds [Isomyricitrin, HK-8; quercetin-8-(2''-pyrrolidione-5''-yl)-3′-*O*-β-D-glucopyranosid, HK-E3] suppressed osteoclastogenesis in murine Raw264.7 cells. HK-11 directly inhibited MM cells (ARP1 and H929) proliferation and induced G0/G1 cell cycle arrest, which may have involved the suppressing β-catenin protein, increasing expressions of IL-6 and TNF-α, as well as activating mature TGF-β1 and some other metabolic pathways.

Conclusion: These results of the present study indicated that the bio-active ingredients of HKC exerted protective effects on MM mouse survival through promoting osteoblastogenesis and suppressing osteoclastogenesis, thus improving the bone marrow microenvironment to inhibit MM cell proliferation.

Keywords: *Abelmoschus manihot L.*, Huangkui capsule, flavonoid extracts, multiple myeloma, osteoclast, osteoblast

Introduction

Multiple myeloma (MM), as the second most common haematological malignancy worldwide, is incurable and characterized by the accumulation of monoclonal plasma cells in the bone marrow (BM).[1] Malignant plasma cells expand in the BM, where they grow, develop, acquire resistance to apoptosis and eventually cause symptomatic MM (that is CRAB: High calcium, renal impairment, anemia and bone lesions).[2] The BM microenvironment (BMM), also named the BM niche, is comprised of a cellular compartment (e.g., osteoclasts, osteoblasts, stromal cells and endothelial cells) and a non-cellular compartment, including the extracellular matrix (ECM) and the liquid milieu (containing cytokines, growth factors and chemokines).[3,4] Although a great number of genetic and epigenetic mutations may occur, almost all MM plasma cells are strictly dependent on the BMM, between which the complex interaction influences MM development and prognosis.[4]

Abelmoschus manihot (Linnaeus) Medicus (Malvaceae) (Chinese name: *Huang Shu Kui*) is widely distributed in China and India. It is a flowering plant of the mallow family Malvaceae. The flowers of *Abelmoschus manihot* (*Flos A. manihot*) have been used as a traditional Chinese medicine, which has been prescribed as "an effective herb in the treatment of various malignant sore, cellulitis and burns" in the *Compendium of Materia Medica* compiled by Shizhen Li (1518–1593 CE) for more than four centuries. Huangkui capsules (HKCs), produced by the Jiangsu Suzhong Pharmaceutical Group (Taizhou, Jiangsu, China), are single-plant-based drugs extracted from the dry corolla of *Flos A. manihot*. In 1999, HKCs received regulatory approval from China State Food and Drug Administration as a Class III drug (approval no. Z19990040) for the treatment of chronic glomerulonephritis[5–7] and other inflammatory diseases.[8,9] Various flavonoids have been determined as the major chemical constituents of *Flos A. manihot* via spectroscopy,[10] chromatography,[11] and high-performance liquid chromatography (HPLC).[12] The absorption and metabolites of these flavonoids following oral administration have been previously studied in rats with adriamycin-induced chronic kidney disease.[13,14]

However, pre-clinical and pharmacological researches using the flavonoid extracts of *Flos A. manihot* have mainly focused on kidney disease or nephritis with limited reports assessing hepatoprotective effects.[15,16] Furthermore, few studies have assessed its therapeutic effect on MM. Therefore, with the consideration that renal impairment is one of the key symptoms of MM patients, the current study hypothesized that flavonoid extracts from *Flos A. manihot* may improve the survival rate of patients with incurable MM and exert protective effects.

To address the aforementioned aims, the present study established a murine MM model to verify the therapeutic effects of HKC. Various analyses were also performed to determine the effect of *Flos A. manihot* bioactive compounds on MM cell proliferation, osteoblast cell differentiation and osteoclastogenesis.

Materials and Methods

Cell Lines and Cultures

ARP1 and H929 human MM cell lines and the murine MM cell line, 5TMM3VT, were purchased from the Cell Resource Center of the Shanghai Institute of Biochemistry and Cell Biology at the Chinese Academy of Sciences. Cells were cultured in RPMI 1640 (Biological Industries, Beit Haemek, Israel), supplemented with 10% fetal bovine serum (FBS; Biological Industries, Israel) and 1% penicillin/streptomycin (P/S).

The pre-osteoblast murine cell line MC3T3-E1 was purchased from the Cell Resource Center of the Shanghai Institute of Biochemistry and Cell Biology at the Chinese Academy of Sciences, and cultured in alpha modified Eagle's medium (α-MEM; Biological Industries, Israel) supplemented with 10% FBS (Biological Industries, Israel) and 1% (P/S). Cells were routinely subcultured using 0.05% trypsin/EDTA (Biological Industries, Israel) upon reaching 80–90% confluence.

The pre-osteoclast murine cell line Raw264.7 was purchased from the ATCC and cultured in Dulbecco's modified Eagle medium (DMEM; Biological Industries, Israel), supplemented with 10% FBS (Biological Industries, Israel) and 1% P/S. After reaching 80–90% confluence, cells were routinely subcultured using 0.05% trypsin/EDTA (Biological Industries, Israel). All cells were maintained at 37°C in a humidified atmosphere of 5% CO2. Medium was changed every 2 days.

Reagents and Chemicals

HKC was purchased from Suzhong Pharmaceutical Group Co., Ltd. (Taizhou, China) and HKC powder (batch no. 18102704) was dissolved in distilled water (HKC suspension) and stored at 4°C before use. Nine compounds were extracted from the flowers of *Abelmoschus manihot* and each was dissolved in dimethyl sulfoxide (DMSO). The quality of extracts

was determined via fingerprint analysis by HPLC as described previously.[17] As presented in Table 1, the nine flavonoid components were as follows: HK-2 (Hyperin/Hyperoside; C AS, 482-36-0), HK-3 (Cannabiscitrin; CAS, 520-14-9), HK-4 (4H-1-Benzopyran-4-one, 2-[3-(β-D-galactopyranosyloxy)-4-hydroxyphenyl]-3,5,7-trihydroxy-; CAS, 1189335-34-9), HK-7 (Floramaroside F; CAS, 1487423-58-4), HK-8 (Isomyricitrin; CAS, 19833-12-6), HK-9 (Ampelopsin; CAS, 27200-12-0), HK-11 (3-*O*-kaempferol-3-*O*-acetyl-6-*O*-(p-coumaroyl)-β-D-glucopyranoside; CAS, 557765-92-1), HK-B10 (8-(2"-pyrrolidione-5"-yl)-quercetin; CAS, 1174048-57-7), HK-E3 (quercetin-8-(2"-pyrrolidione-5"-yl)-3′-*O*-β-D-glucopyranosid; CAS, 2230816-80-3).

MTT Assay

MM cell proliferation was measured by performing a colorimetric 3-(4,5-dimethylthiazol-2-yl)-2,5-diphenyltetrazolium bromide (MTT) assay according to the manufacturer's protocol (Beyotime Institute of Biotechnology, Shanghai, China). ARP1 and H929 cells were seeded in 96-well plates at a density of 10,000 cells/cm^2 per well and then cultured with media containing different concentrations of the nine aforementioned compounds. After incubation for 48 h, MTT solution (5 μg/μL) was added to each well (20 μL) and incubated for 4 h in a humidified incubator at 37°C with 5% CO_2. MTT and media were subsequently removed and 150 μL DMSO was added to each well. After vibration for 1 min, absorbance was measured using a microplate reader at 562 nm (Thermo Fisher Scientific, Inc., USA).

Flow Cytometry

Flow cytometry was performed to determine the effect of HK-11 on the cell cycle distributions of ARP1 and H929 cells. Cells were treated with HK-11 for 48 h, after which they were collected, fixed with 70% ethanol and incubated overnight at −20°C. Cells were then washed with PBS and stained with 1 mg/mL Propidium Iodide (Sigma-Aldrich; Merck KGaA) in the presence of RNase A solutions (Sigma-Aldrich; Merck KGaA). At least 10,000 events were acquired by using guava easyCyte (Guava Technologies, Hayward, CA, USA). Data were analyzed using FlowJo software (Tree Star Corp, Ashland, OR, USA).

Animal Experiments

The 8-week-old male/female C57BL/KaLwRij mice (n = 9 per group) used for in vivo studies were injected intravenously with 5TMM3VT (1x10^6 cells per mouse). Treatments with HKC started from the next day (3 times/week), and continued until the mice were dead. All animal procedures were conducted in accordance with government-published recommendations for the Care and Use of Laboratory Animals and were approved by the Institutional Ethics Review Boards of Nanjing University of Chinese Medicine (approval no. ACU170501).

Alizarin Red Staining Assays and Osteoblast Mineralization

MC3T3-E1 cells were seeded at a density of 5000 cells/well in 12-well plates. When cells reached 70–80% confluence, they were divided into 3 groups: A normal control group (NC), a positive control (PC) group, and an experimental group. The NC group was cultured in α-MEM complete medium and the PC group was cultured in osteogenic induction medium (α-MEM complete medium; osteogenic inducer, β-glycerophosphate 10 mmol/l, ascorbic acid 50 mg/l). With use of the osteogenic induction solution, the experimental group was divided into 4 further

Table 1 Characteristics of Flavonoid Compounds in Huangkui Capsule from Flowers of Abelmoschus Manihot (L.) Medik

Number	Name	CAS ID	Molecular Formula	Molecular Weight
HK-2	Hyperin	482-36-0	$C_{21}H_{20}O_{12}$	464
HK-3	Cannabiscitrin	520-14-9	$C_{21}H_{20}O_{13}$	480
HK-4	4*H*-1-Benzopyran-4-one, 2-[3-(β-D-galactopyranosyloxy)-4-hydroxyphenyl]-3,5,7-trihydroxy-	1189335-34-9	$C_{21}H_{20}O_{12}$	464
HK-7	Floramaroside F	1487423-58-4	$C_{23}H_{22}O_{14}$	534
HK-8	Isomyricitrin	19833-12-6	$C_{21}H_{20}O_{13}$	480
HK-9	Ampelopsin	27200-12-0	$C_{15}H_{12}O_8$	320
HK-11	3-*O*-kaempferol-3-*O*-acetyl-6-*O*-(*p*-coumaroyl)-*β*-D-glucopyranoside	557765-92-1	$C_{32}H_{28}O_{14}$	636
HK-B10	8-(2"-pyrrolidione-5"-yl)-Quercetin	1174048-57-7	$C_{19}H_{15}NO_8$	385
HK-E3	Quercetin-8-(2"-pyrrolidione-5"-yl)-3′-*O*-β-D-glucopyranoside	223016-80-3	$C_{25}H_{25}NO_{13}$	547

groups that were treated with varying concentrations of HK-2 (5 μM and 50 nM), HK-3 (5 μM and 50 nM), HK-11 (5 μM and 50 nM), HK-B10 (5 μM and 50 nM), respectively. Osteogenic medium was refreshed every 3 days for 4 weeks. After 28 days, cells were washed in triplicate with PBS and fixed with 4% paraformaldehyde for 15 min at room temperature. Fixed cells were washed 3 times with distilled water and stained with 2% Alizarin Red S solution (pH 4.2) for 30 min at 37°C. Stained cells were subsequently washed with distilled water 3 times and air-dried in the dark before imaging.

Tartrate-Resistant Acid Phosphatase (TRAP) Activity Staining

Raw264.7 cells were seeded in 48-well plates at a density of 5000 cells/well in DMEM medium supplemented with recombinant murine sRANKL (Peprotech, USA) and M-CSF (Peprotech, USA) on day 2. The medium was refreshed every 3 days and treated with HK-8 (50 and 5 μM) and HK-E3 (50 and 5 μM). After 6 days, cells were stained for TRAP activity using the Leukocyte Tartrate-Resistant Acid Phosphatase kit (Sigma-Aldrich; Merck KGaA).

Transcriptomic RNA Sequencing

RNA-sequencing and sample analysis was performed by MicroAnaly (Shanghai, China). mRNA was extracted from murine or human total RNA following the removal of rRNA. After constructing an RNA-sequencing library, the Illumina NovaSeq 6000 platform was utilized for PE150 sequencing. Data were analyzed using strict data quality controls to identify several differentially expressed genes (DEGs).

Reverse-Transcription Quantitative PCR (RT-qPCR)

RT-qPCR was performed to detect the mRNA levels of IL-6, TNF-α and VEGF in accordance with MIQE guidelines. Total RNA from ARP1 and H929 cells was extracted using TRIeasy (Yeasen, Shanghai, China). The RNA yield was determined using an A260/A280 ratio with NanoDrop ND-1000 (Thermo Fisher Scientific, Inc., USA) and integrity was assessed using 1% agarose gel. Subsequently, the HiScript III RT SuperMix kit (Vazyme, Nanjing, China) was used to reverse transcribe 500 ng isolated RNA into cDNA. qPCR was then performed with a SYBR Green Supermix kit (Bio-Rad Laboratories, Inc., Hercules, CA, USA) in accordance with the manufacturer's protocol. PCR amplifications were performed and a dissociation stage was added for melting curve analysis to determine amplicon specificity. Samples were detected in triplicate using RNA preparations from three independent experiments. The relative expression of mRNA was calculated using the $2^{-\Delta\Delta cq}$ method,[18,19] and the fold change of each gene expression was normalized to that of GAPDH. The following primer sequences with amplification efficiency between 90% and 110%, were used: IL-6, Forward: 5′-GTAGTGAGGAACAAGCCAGAGC-3′ and Reverse: 5′-TACATTTGCCGAAGAGCCCT-3′; TNF-α, F: 5′- TCTACTCCCAGGTCCTCTTCAAG-3′ and R: 5′- GGAAGACCCCTCCCAGATAGA-3′; VEGF, F: 5′-GGAGGGCAGAATCATCACGA-3′ and R: 5′- GCTCATCTCTCCTATGTGCTGG-3′; GAPDH, F: 5′- GACACCCACTCCTCCACCT -3′ and R: 5′- ATGAGGTCCACCACCCTGT -3′.

Western Blotting

MM cells, osteoblast lysates and osteoclast lysates were analyzed via Western blotting using standard methods. The specific experimental protocols involving osteoblast and osteoclast differentiation were the same as described previously.[20–22] At day 14 after the start of osteoblast differentiation, cells were lysed in RIPA (Beyotime Institute of Biotechnology, China). At day 6 after following the start of osteoclast differentiation, cells were lysed in RIPA (Beyotime Institute of Biotechnology, China). Following treatment with HK-11 for 48 h, MM cells were lysed in RIPA (Beyotime Institute of Biotechnology, China). Cell lysates (40 μg per lane) were separated using 10–15% Novex Bis-Tris SDS-acrylamide gel (Invitrogen, Life Technologies, USA), transferred onto nitrocellulose membranes (Invitrogen, Life Technologies, USA) and immunoblotted with the following primary antibodies: β-catenin (1:1000; cat. no. sc-7199, Santa Cruz Biotechnology, Inc., USA), TGF-β1(1:1000; cat. no. ab92486, Abcam, USA), β-actin (1:1000; cat. no. cst 4967L, Cell Signaling Technology, USA), GAPDH (14C10) Rabbit mAb (1:1000; cat. no.2118, Cell Signaling technology, USA). Samples were then treated with the following secondary antibodies: HRP-conjugated anti-mouse IgG (1:10,000; cat. no. sc-2005, Santa Cruz Biotechnology, USA) or HRP-conjugated anti-rabbit IgG (1:10,000; cat. no. sc-2004, Santa Cruz Biotechnology, USA). Chemiluminescence was detected using a Tanon™ High-sig ECL Western Blotting Substrate (Tannon, China).

Statistical Analysis

Data were analyzed using GraphPad Prism 5.0 software (GraphPad Software Inc., La Jolla, CA, USA) and

presented as the mean ± standard deviation. Significant differences were analyzed using Mann–Whitney U nonparametric tests and one-way ANOVA for multiple comparisons. P<0.05 (*), P<0.01 (**) and P<0.001 (***) were considered to indicate statistically significant differences.

Results

HKC Improves Survival Rate of MM-Prone Mice

HKC was orally administered to MM mice (3.75 g/kg body weight, 3 times/week) once the 5TMM3VT syngeneic MM-prone model was established (Figure 1A). The results revealed that control MM mice rapidly deteriorated from day 37 until all mice were dead by day 68. However, HKC treated MM-prone mice exhibited prolonged survival rates up to ~3 months (P=0.0284; Figure 1B).

Flavonoid Compounds Promote Osteoblastogenesis and Suppress Osteoclastogenesis in Murine Cell Lines

To further assess the bio-active ingredients of HKC that exert protective effects on MM, nine flavonoid compounds were isolated from *Flos A. manihot*, which have been regarded by previous studies as the primary active components.[8,11–13,21] These include HK-2, HK-3, HK-4, HK-7, HK-8, HK-9, HK-11, HK-B10 and HK-E3 (see detailed information listed in Table 1). As MM cells reside in various BMM components, including stromal cells, osteoblasts, osteoclasts and other non-cellular components, and exhibit a bone-remodeling balance between bone construction (by osteoblast cells) and destruction (by osteoclast cells),[3,4] the current study determined the effects of the nine flavonoid compounds on the development of pre-osteoblast and pre-osteoclast cells.

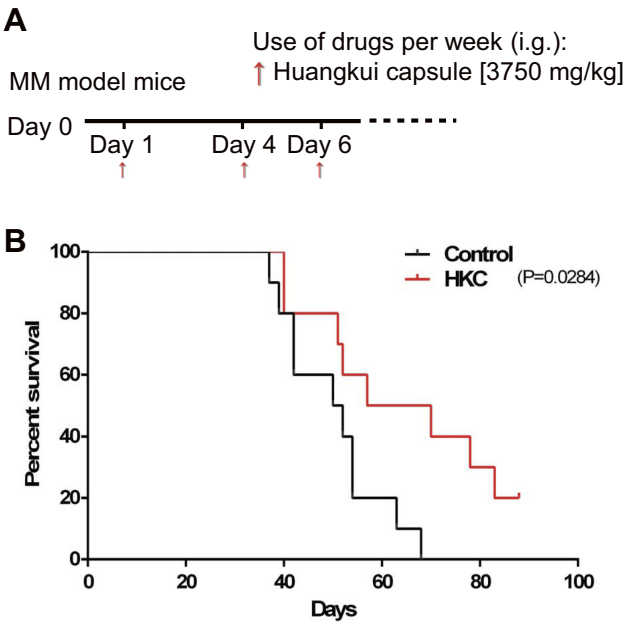

Figure 1 HuangKui capsule improves the survival rates of multiple myeloma-prone C57BL/KaLwRij mice. An MM model was established by injecting 8-week-old male/female C57BL/KaLwRij mice with intravenous 5TMM3VT via the tail vein ($1x10^6$ cells per mouse; n=10 per group). (**A**) Treatment with HKC started from the day after injection (3 times/week) and continued until the mice were dead. (**B**) The 3-month survival curves of MM model mice with or without HKC treatment are presented.

As presented in Figure 2, Alizarin Red Staining of pre-osteoblast murine MC3T3-E1 cells revealed that four compounds (HK-2, HK-3, HK-B10 and HK-11) enhanced the mineralization of differentiated osteoblasts when compared with the PC group (Figure 2A–C). The quantification of staining results (Figure 2D and E) demonstrated that HK-2, HK-3, HK-B10 and HK-11 promoted the differentiation of MC3T3-E1 cells at two different dosages (0.05 and 5 μM).

The current study further assessed the inhibitory effects exerted by the nine flavonoid compounds on pre-osteoclast Raw264.7 cells. TRAP activity results revealed that only HK-8 and HK-E3 could significantly down-regulate the formation of osteoclast in DMEM medium containing recombinant murine sRANKL and M-CSF, when compared to PC group cells (Figure 3A–C). In addition, for either HK-8 or HK-E3 treatment, the dosage at 50 μM has a comparable inhibitory effect with the concentration of 5 μM (Figure 3B and C).

Flavonoid Compounds Trigger Osteoclast Differentiation Pathways in Pre-Osteoclast Raw264.7 Cells

The present study aimed to determine how isolated HK-8 and HK-E3 compounds effectively suppressed osteoclastogenesis, as the overgrowth of MM cells in the BM involves a bone-remodeling process that requires bone destructive osteoclast cells. Raw264.7 cells treated with HK-8 and HK-E3, as well as the CON and PC groups were used for RNA-sequencing. As presented in Figure 4, RNA-sequencing identified 284 unique DEGs between every two groups (|FoldChange| ≥2; FDR value ≤0.05). However, no single gene was significantly altered in each group. The number of upregulated DEGs was ~2–3 fold higher than the number of downregulated DEGs in any two groups, suggesting that other cellular molecules may be directly or indirectly involved in inhibiting of pre-osteoclast differentiation

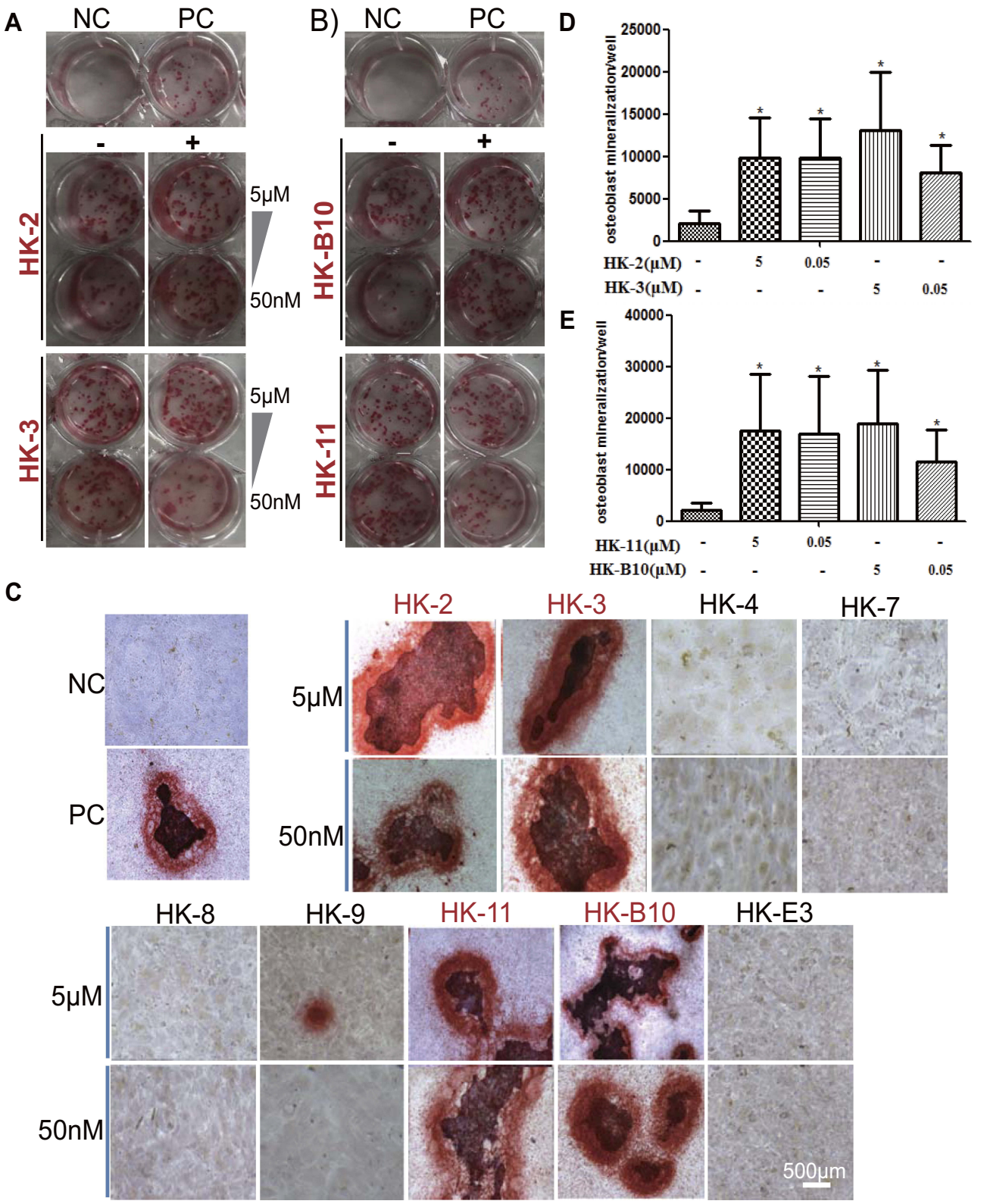

Figure 2 Flavonoid compounds promote the differentiation of the pre-osteoblast murine cell line, MC3T3-E1. (**A** and **B**) MC3T3-E1 cells were seeded in 12-well plates and were cultured in osteogenic medium containing flavonoid compounds for 4 weeks prior to Alizarin red staining. Medium containing or not containing 50 μg/mL ascorbic acid and 10mM β-glycerophosphate was used as a negative control (NC) and positive control (PC), respectively. Two dosages (5 μM and 50 nM) of (**A**) HK-2 and HK-3, (**B**) HK-11 and HK-B10 were applied. Representative results of Alizarin red staining for the nine flavonoid compounds are presented. Scale bar, 500 μm. (**C**) The quantification of positive mineralized cells following (**D**) HK-2 and HK-3 treatment and (**E**) HK-11 and HK-B10 treatment are presented. Scale bar, 500 μm. *P<0.05.

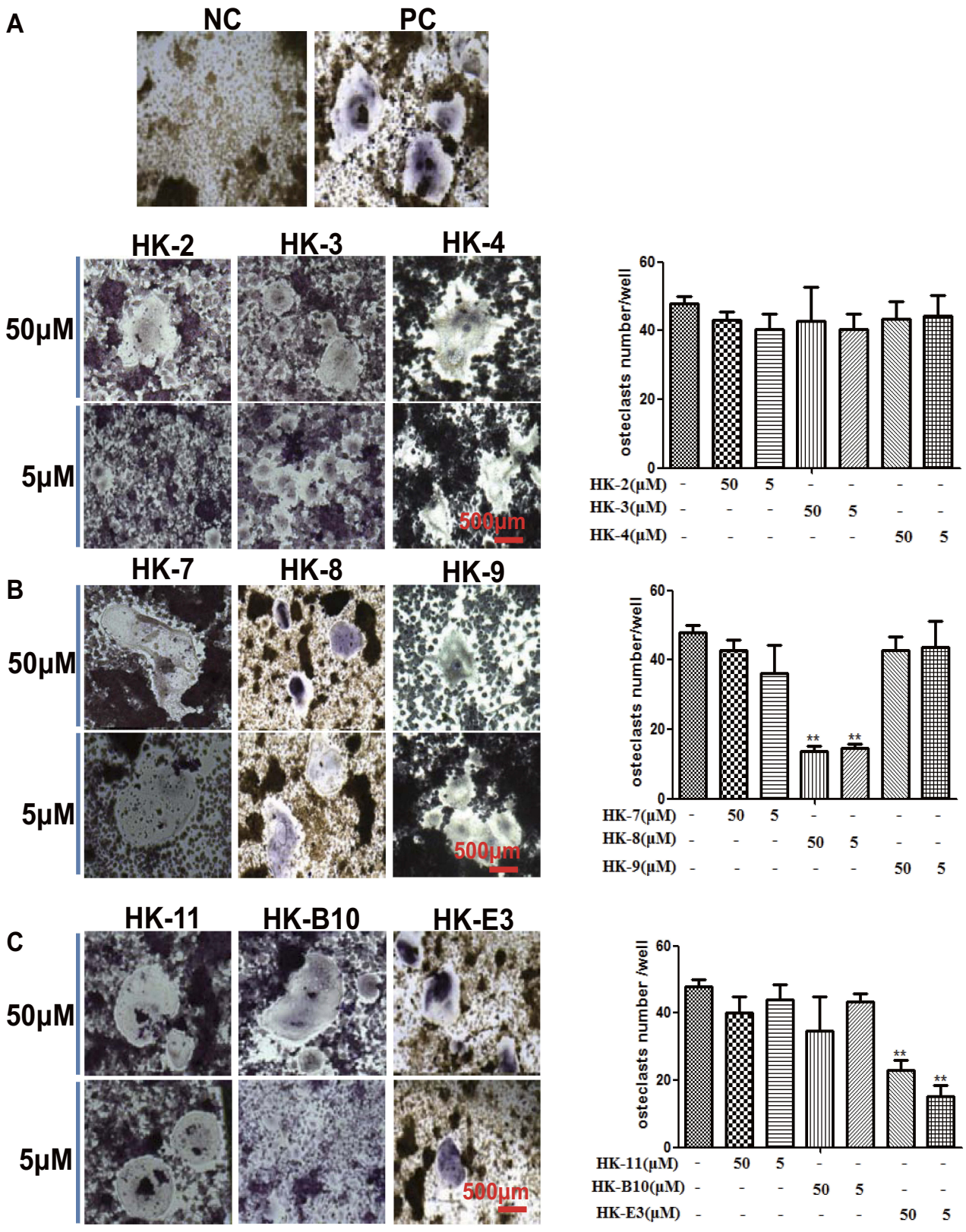

Figure 3 Flavonoid compounds inhibit differentiation of pre-osteoclast murine cell line. RAW264.7 cells were cultured in DMEM containing recombinant murine sRANKL and M-CSF (Positive control) and treated with flavonoid compounds for 6 days, after which cells were stained using a Leukocyte Tartrate-Resistant Acid Phosphatase kit. The quantification of TRAP osteoclast staining is presented following treatment with (**A**) HK-2, HK-3 and HK-4, (**B**) HK-7, HK-8 and HK-9 and (**C**) HK-11, HK-B10 and HK-E3. NC, negative control; Scale bar, 500 μm. **P<0.01.

A

RNA-seq for Raw264.7 cells post HK-8, HK-E3 treatment

DEG found Groups			UP
PC vs CON	24	8	16
HK-8 vs CON	172	43	129
HK-8 vs PC	**149**	**52**	**97**
HK-E3 vs CON	177	44	133
HK-E3 vs PC	**124**	**40**	**84**
HK-8 vs HK-E3	11	6	5

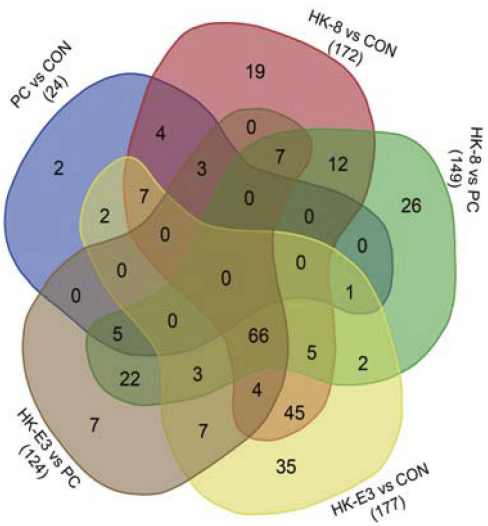

B

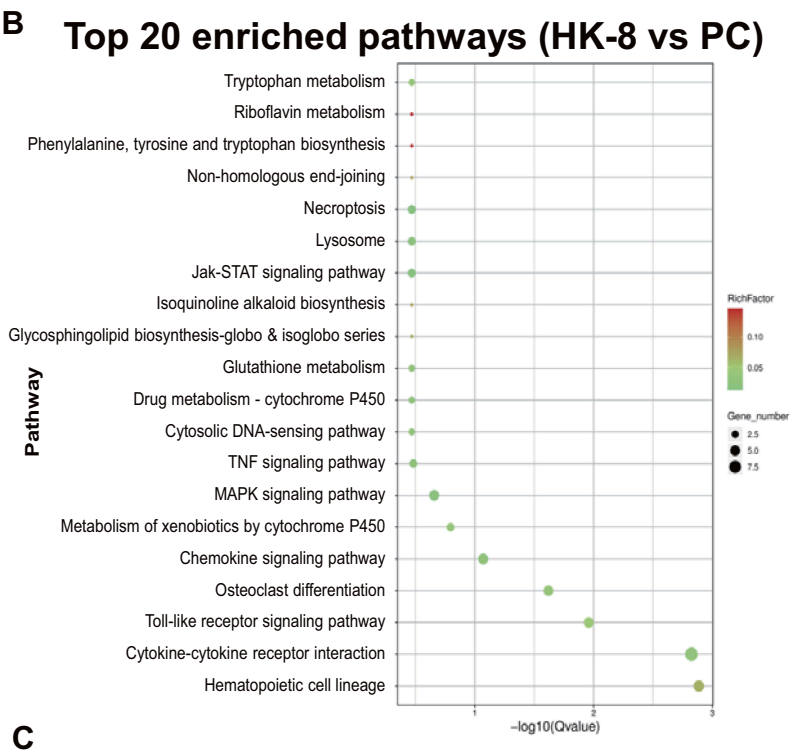

C

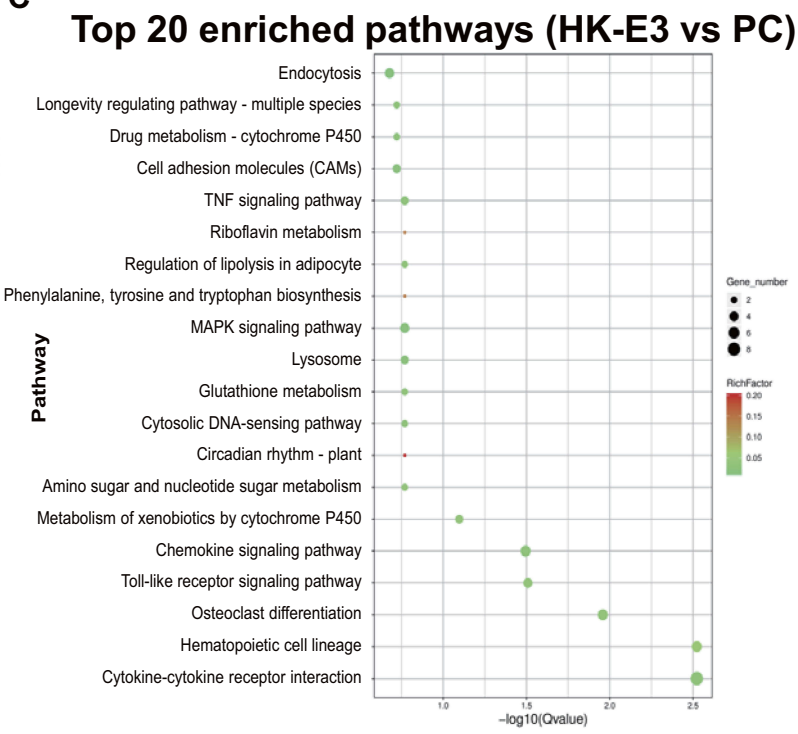

Figure 4 RNA-sequencing reveals differentially expressed genes (DEGs) and enriched KEGG pathways in murine Raw264.7 cells following treatment with HK-8 and HK-E3. (**A**) The DEGs identified in NC (negative control), PC (Positive control), HK-8 and HK-E3 groups in RAW264.7 cells are presented in Venn diagram, as identified via RNA-sequencing. KEGG pathway enrichment analyses for (**B**) HK-8 and (**C**) HK-E3 groups are shown as scatter plots. The Y-axis represents the 20 enriched pathways (based on a corrected P-value) and the X-axis represents the richness factor reflecting the proportion of DEG in any given pathway. The number of DEGs in the pathway is indicated by the circle area. The circle color represents the range of the corrected P-values.

(Figure 4A). DEG KEGG (Kyoto Encyclopedia of Genes and Genomes) pathway enrichment analysis revealed that many different pathways were altered. The top 20 ranked pathways in HK-8 vs PC and HK-E3 vs PC groups are presented in Figure 4B and C. For example, osteoclast differentiation (ko04380), chemokine signaling pathway

(ko04062), hematopoietic cell lineage (ko04640), TNF signaling pathway (ko04668), riboflavin metabolism (ko00740), drug metabolism-cytochrome P450 (ko00982), metabolism of xenobiotics by cytochrome P450 (ko00980) and glutathione metabolism (ko00480) were enriched in both groups. Additionally, cell adhesion molecules (CAMs) (ko04514) involved in the processing of environmental information and cell communication were enriched in HK-E3 vs PC (Figure 4C).

HK-11 Directly Inhibits MM Cells Proliferation and Downregulates β-Catenin Signaling

To determine the direct effect of the nine flavonoid extracts on MM cells proliferation, the present study performed an MTT assay for two human MM cells (ARP1 and H929) following treatment with each extract at eight different dosages (3.125–200 μM). The half-maximal inhibitory concentration (IC50) of each treatment was then assessed (Table 2). The results revealed that six of the nine compounds (excluding HK-8, HK-B10 and HK-E3) exerted varying inhibitory effects on MM cell proliferation. Among these, HK-11 exerted the most significant inhibitory effect on the proliferation of both ARP1 and H929 cells. HK-11 was therefore selected for future study (Figure 5A). The results of flow cytometry confirmed that HK-11 treatment-induced ARP1 and H929 cell cycle arrest at the G0/G1 phase, decreasing the percentage of S phase cells (Figure 5B). A previous study has demonstrated that the WNT/β-catenin signaling pathway was involved in the growth and proliferation of MM cells. The study further revealed that β-catenin could be stabilized by Lithium chloride (LiCl) treatment, thus activating the WNT/β-catenin pathway.[22] The present study, therefore, assessed β-catenin protein levels in MM cells following treatment with HK-11. Western blotting revealed that HK-11 treatment downregulated β-catenin protein levels, particularly in H929 cells (Figure 5C). Additionally, this inhibitory effect appeared to be reversed following induction with higher concentration of LiCl (Figure 5D).

Table 2 The Half Maximal Inhibitory Concentration (IC50, μM) of Flavonoid Compounds in HKC for Two MM Cell Lines

Cell Lines	ARP1	H929
HK-2	113.2	92.75
HK-3	101.1	89.58
HK-4	220.7	109.8
HK-7	147.7	195.8
HK-8	N/A	N/A
HK-9	207.7	352
HK-11	57.16	55.88
HK-B10	N/A	N/A
HK-E3	N/A	N/A

Abbreviation: N/A, Not available.

RNA Profiling and Enriched KEGG Pathways in MM Cells Following HK-11 Treatment

To further investigate the potential mechanisms of HK-11's inhibitory effect on MM cell proliferation, RNA-sequencing was performed in H929 and ARP1 cells (Figure 6). According to the altered gene expression pattern, the 68 DEGs identified in HK-11 vs H929 group could be clustered into three sub-clusters, the majority of which were down-regulated (Figure 6A). However, in the HK-11 vs ARP1 group, 32 DEGs were clustered into four sub-clusters, the majority of which were upregulated (Figure 6B). The top 20 enriched KEGG pathways of the two groups were presented as scatter plot. Among them, RNA polymerase (ko03020) was ranked as the most enriched pathway in H929 cells (DEG, *MSTRG.437* as one of core subunits of PolII, *MSTRG.448* as PolIII specific subunit). The results also revealed enriched metabolism/digestive pathways, including those of sulfur metabolism (ko00920), glycosaminoglycan biosynthesis-chondroitin sulfate/dermatan sulfate (ko00532), protein digestion and absorption (ko04974), immune system-related Cytosolic DNA-sensing pathway (ko04623) and NOD-like receptor signaling pathway (ko04621) (Figure 6C). In the HK-11 vs ARP1 group, the present study revealed that aminoacyl-tRNA biosynthesis (ko00970) was the most significant pathway (DEG, *MSTRG.176* and *MSTRG.138* both involved in Valine-tRNA biosynthesis), with various other replication and repair pathways also being of significance, including those of base excision repair (ko03410), DNA replication (ko03030), homologous recombination (ko03440), mismatch repair (ko03430) and nucleotide excision repair (ko03420). The results also demonstrated that certain biosynthesis and metabolism pathways were enriched, including those of amino arginine and proline metabolism (ko00330), various types of N-glycan biosynthesis (ko00513), glycerophospholipid metabolism (ko00564), pyrimidine metabolism (ko00240; Figure 6D).

To confirm the effect of HK-11 on MM cells, various growth factors were assessed in the present study, including

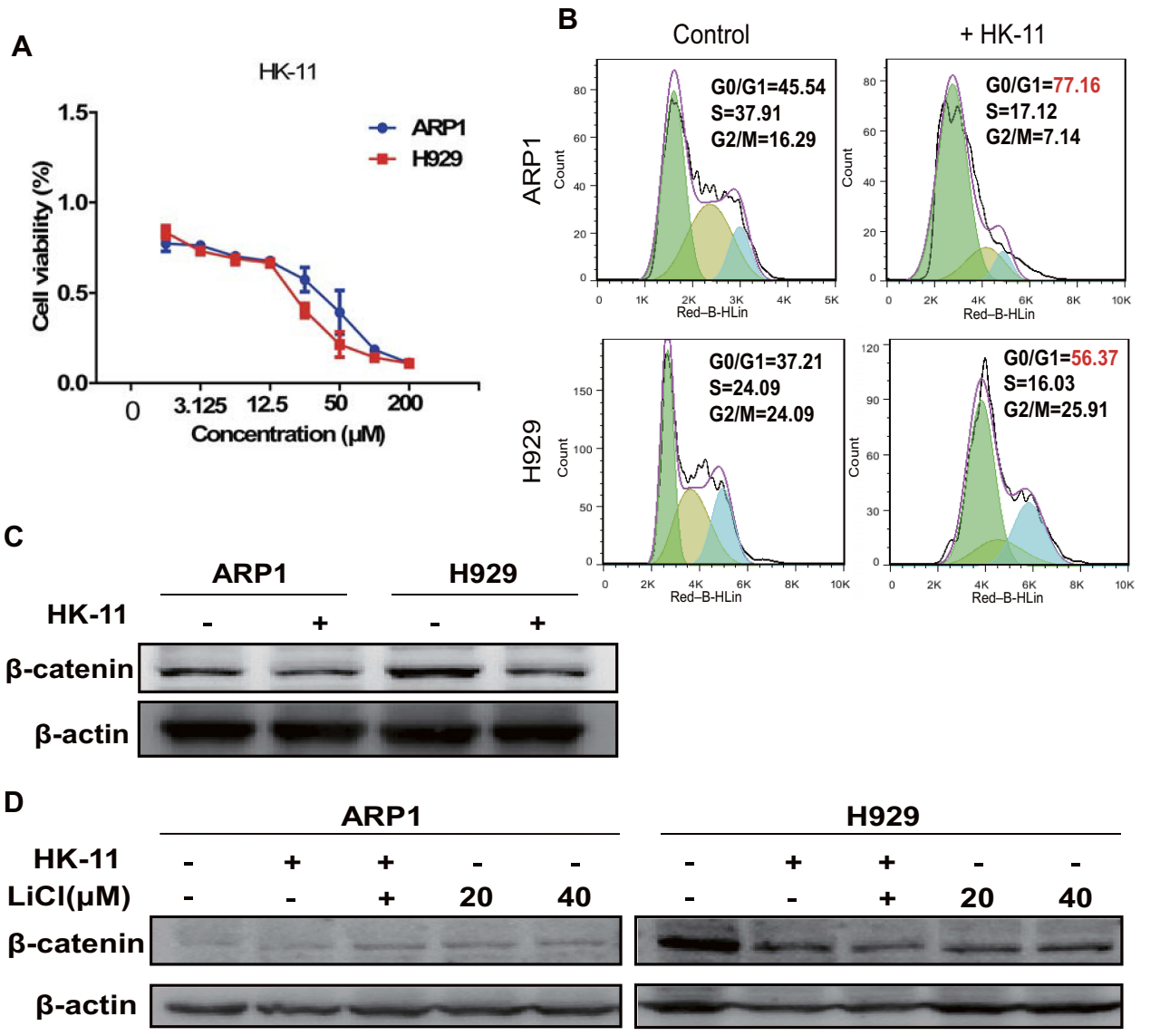

Figure 5 HK-11 treatment inhibits the proliferation of human MM cells. (**A**) The cell proliferation of two MM cell lines (ARP1 and H929) following treatment of eight dosages of HK-11 (3.125–200 μM) was assessed using an MTT assay. (**B**) Flow cytometry was also performed following Propidium Iodide/RNase staining in ARP1 and H929 cell with or without HK-11 treatment. The results demonstrated an increased proportion of cells in the G0/G1 phase. (**C**) Decreased levels of β-catenin proteins were detected after HK-11 treatment in ARP1 and H929 cells. (**D**) HK-11 attenuated the activation of LiCl-induced β-catenin signaling.

cytokine interleukin-6 (IL-6), Tumor Necrosis Factor alpha (TNF-α), Vascular Endothelial growth Factor (VEGF) and Transforming growth factor-beta (TGF-β), which were believed to play key roles in the cell proliferation and differentiation and cell–cell interaction residing in the BMM (Figure 7). The results of RT-qPCR indicated that IL-6 and TNF-α RNA levels were significantly altered >10-fold following HK-11 treatment in H929 cells. However, VEGF levels were downregulated to ~40%, although the difference was not statistically significant. A similar gene expression trend was observed in H929 cells, but to a lesser extent (Figure 7A). Furthermore, protein levels of mature TGF-β1 were increased in both ARP1 and H929 cells. However, the full-length precursor protein exhibited varied changes depending on the cell types used, with upregulation been demonstrated in ARP1 cells and down-regulation in H929 post-HK-11 treatment (Figure 7B).

Discussion

Flavonoids are the major active components isolated from the traditional Chinese herb, *Abelmoschus manihot* L. Medic.[8,11–13,23] Previous studies have reported their successful use in the treatment of kidney and inflammatory diseases.[5–7,9,14] In the current study, in vivo results

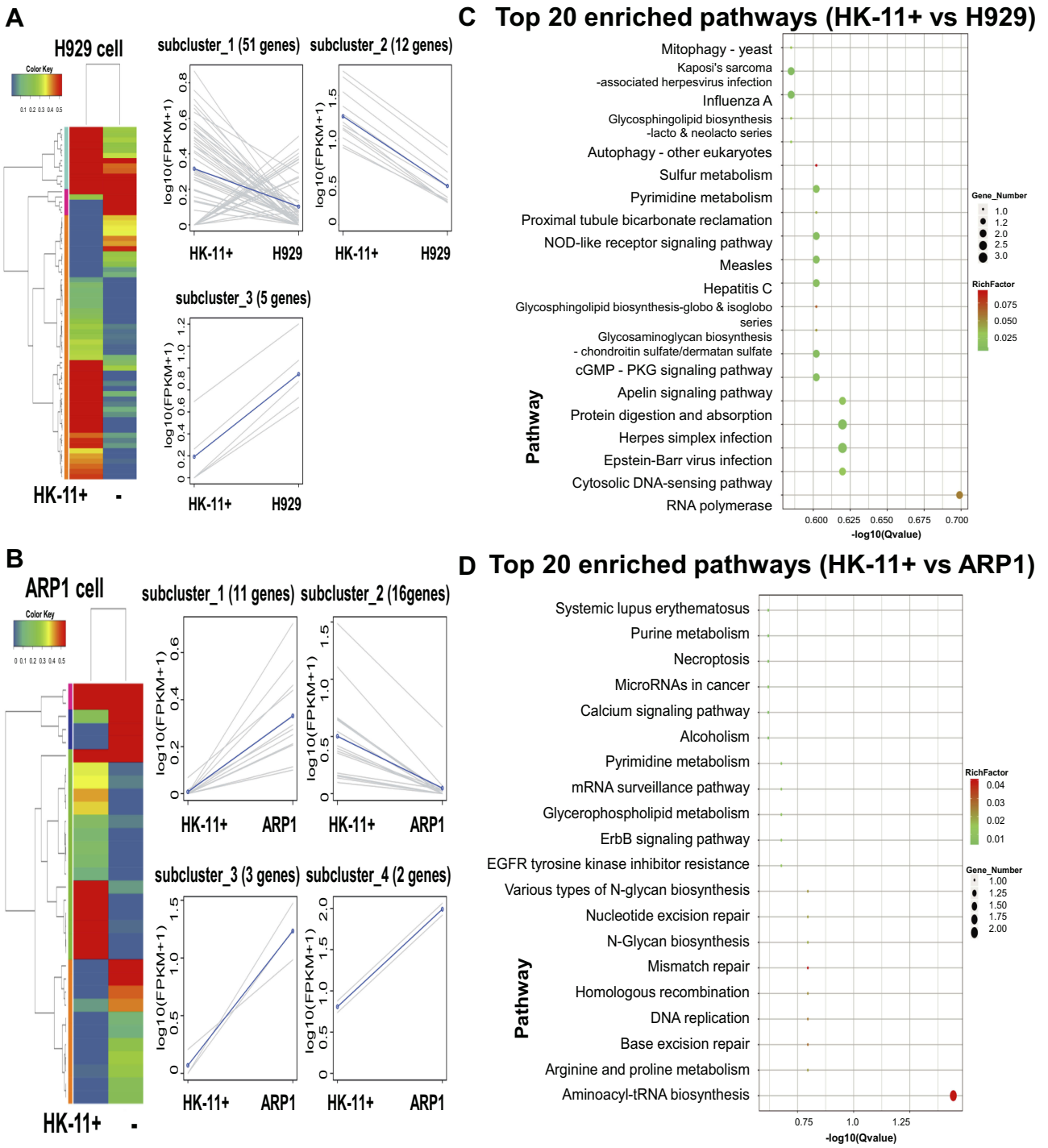

Figure 6 RNA-sequencing results revealed differentially expressed genes (DEGs) and enriched KEGG pathways in MM cells following HK-11 treatment. DEGs were identified via RNA-sequencing in (**A** and **C**) H929 and (**B** and **D**) ARP1 cells following HK-11 treatment. These DEGs were subsequently used for gene clustering and pathway enrichment analysis. (**A**) Three sub-clusters were identified in H929 cells and (**B**) four sub-clusters were identified in ARP1 cells. The top 20 enriched KEGG pathways found in (**C** and **D**) HK-11 vs H929 and HK-11 vs ARP1 groups are presented as scatter plots. The Y-axis represents 20 enriched pathways (based on corrected P-value) and the X-axis represents the richness factor reflecting the proportion of DEG in any given pathway. The number of DEGs in the pathway is indicated by the circle area. The circle color represents the range of the corrected P-values.

revealed that the oral administration of HKC improved the survival rates of 5T MM syngeneic mice (Figure 8). To the best of our knowledge, the current study is the first to report the effects of HKC, a modern Chinese patent medicine, on MM. The results of which indicated that HKC may be a promising treatment for human MM. However,

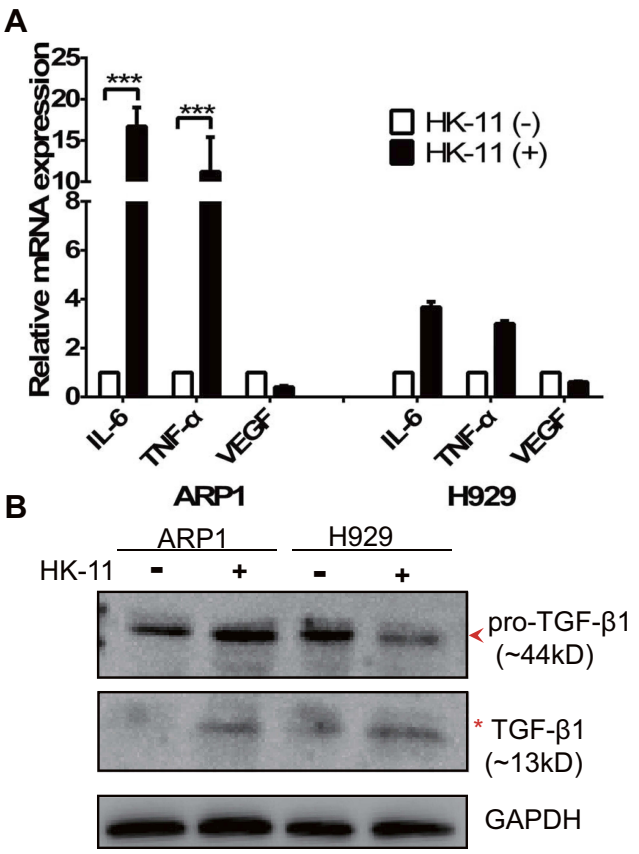

Figure 7 HK-11 modulates various growth factors and regulates TGF-β1 signaling in MM cells. (**A**) RT-qPCR was performed to assess the RNA expressions of IL-6, TNF-α and VEGF. GAPDH was used as an internal control. ***P<0.001. (**B**) Western blotting results show the full-length (arrowhead) and mature TGF-β1 (star) proteins.

further studies are required to determine the underlying mechanism used by the bioactive compound that exerts the desired effect.

The results of the current study demonstrated that of the 9 flavonoid compounds assessed, HK-8 and HK-E3 suppressed the osteoclastogenesis of mouse Raw264.7 cells (Figure 3). Additionally, HK-2, HK-3, HK-11 and HK-B10 promoted pre-osteoblast murine MC3T3-E1 cell differentiation (Figure 2). These results indicated that the flavonoid compounds derived from *Flos A. manihot* may exert protective effects on MM by improving the BMM, since MM cell overgrowth in the BM involves bone-remodeling with bone destructive osteoclast cells. The following pathways were determined to be enriched following RNA-sequencing and KEGG analysis (Figure 4): osteoclast differentiation (ko04380), chemokine signaling pathway (ko04062), hematopoietic cell lineage (ko04640), TNF signaling pathway (ko04668) and Cell adhesion molecules (ko04514), therefore, these pathways involved in environmental information processing and cell–cell interaction were to some extent supporting the reports of HKC's anti-inflammatory effects.[5–7,9,14] Additionally, the enriched pathways of riboflavin metabolism (ko00740), drug metabolism – cytochrome P450 (ko00982), metabolism of xenobiotics by cytochrome P450 (ko00980) and glutathione metabolism (ko00480) may reflect the intermediate processes of first metabolite transformation from the flavonoid extracts from *Flos A. manihot*. According to previously performed experiments on rats, the flavonoid extracts of *Flos A. manihot* were rapidly absorbed and reached peak blood plasma concentrations within 20–30 min after oral administration.[23] Furthermore, hyperoside (also known as hyperin, HK-2 in this study), quercetin, isoquercitrin and quercetin-3′-*O*-glucoside can be absorbed into the plasma as flavonoid aglycones and glycosides, which can be methylated and glucuronidated following deglycosylation.[13] Recently, it was determined via UPLC-MS (ultra-performance liquid chromatography/quadrupole time-of-flight mass spectrometry) that the primary active components of *Flos A. manihot* can be transformed into glucuronide–sulphate conjugates in vivo.[25] The present study also identified enriched pathways of sulfur metabolism (ko00920), glycosaminoglycan biosynthesis-chondroitin sulfate/dermatan sulfate (ko00532) in H929 human MM cells following treatment with HK-11 (Figure 6C). Furthermore, N-Glycan biosynthesis (ko00510), various types of N-glycan biosynthesis (ko00513) and glycerophospholipid metabolism (ko00564) were enriched in human MM ARP1 cells (Figure 6D). It is hypothesized that the flavonoids absorbed into the blood may contribute to the therapeutic efficacy of *Flos A. manihot* via interacting with MM and osteoblast/osteoclast cells in the bone marrow niche.

Previous studies have reported that the activation of the Wnt/β-catenin signaling pathway plays critical roles in both osteoblastogenesis and osteoclastogenesis.[26–28] The aberrant activation of the Wnt/β-catenin pathway with non-phosphorylated active β-catenin expression in the nucleus could sensitize MM cells to autocrine Wnt ligands and paracrine Wnt emanating from the BMM, thus may contribute to the proliferation, migration, and drug resistance of MM cells (see recent review).[29] The results presented in Figure 5C revealed that β-catenin protein levels were downregulated following HK-11 treatment and that this suppressive effect could be reversed by LiCl, which stabilized β-catenin by inhibiting the kinase activity of Glycogen Synthase Kinase-3, a crucial mediator of the Wnt/β-catenin signaling.[24,30] It has been suggested that the inhibitory effect of HK-11 on β-catenin signaling may be utilized as a potential target for treating MM, as the majority of MM patients exhibit hallmarks of Wnt activation in a ligand-

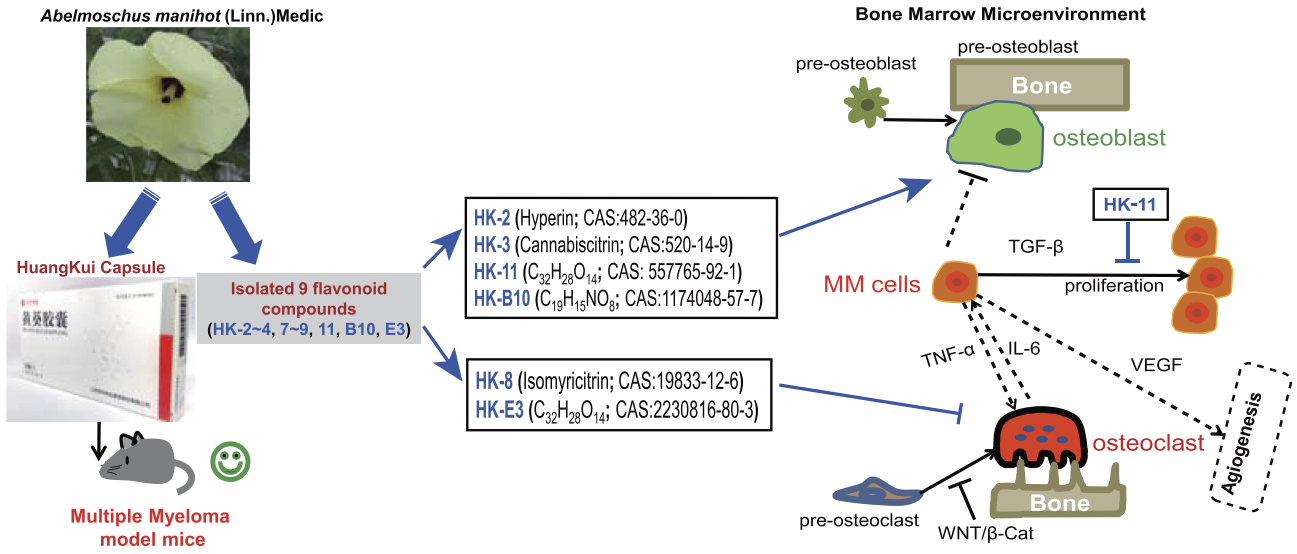

Figure 8 Schematic diagram summarizing the therapeutic effects of the flavonoid ingredients isolated from Abelmoschus manihot (L.) Medik flowers in multiple myeloma. HKC exerts protective effects on the survival of MM mice and may promote osteoblastogenesis and suppress osteoclastogenesis in murine cell lines, thus improving the bone marrow microenvironment. One flavonoid compound was determined to directly inhibit MM cell proliferation by modulating TGF-β1 signaling, inducing IL-6, TNF-α expression and downregulating the β-catenin pathway.

dependent manner, irrespective of the complex genetic heterogeneity.[29] Furthermore, β-catenin is dynamically stored and cleared in MM.[31] Further studies are required to investigate the most effective strategy for targeting canonical Wnt signaling in MM, potentially by inhibiting Wnt/β-catenin activation in the BMM of MM cells.

For many years, the cytokine IL-6 as a central growth factor was regarded to play a pivotal role in the pathogenesis of MM. The cellular sources of IL-6 in MM-infiltrated BM are highly controversial, with their origin usually described as paracrine or autocrine.[32–34] Asides from IL-6, a number of cytokines and growth factors have been demonstrated to be further produced and secreted once the MM cells in communication with bone marrow stromal cell in BMM (see review),[35] such as TNF-α,[36] TGF-β,[37] VEGF.[38] As presented in Figure 7A, RT-qPCR revealed that *TNF-α* and *IL-6* mRNA levels were significantly upregulated in MM cells, while a relatively decreased *VEGF* expression was demonstrated in ARP1 cells following treatment with HK-11. The increased *IL-6* mRNA level may reflect the intricate balancing of IL-6 protein expression between MM cells and their microenvironment, indicating that IL-6 might have intrinsic dual roles in MM tumor cell regulation and BMM remodeling. Similarly, increased TNF-α and decreased VEGF expressions may act in concert with this balancing process. Therefore, HK-11 may serve as a key regulator to stimulate interactions between MM cells and the BMM, contributing to the inhibition of MM proliferation and angiogenesis. Additionally, the increased active protein levels of TGF-β1 in both ARP1 and H929 cells (Figure 7B) further support that HK-11 treatment improves the BMM to inhibit MM cell growth, as TGF-β superfamily members are critical regulators of cell proliferation and differentiation.[39] However, the difference of primary full-length TGF-β1 levels of ARP1 and H929 cells may to some extent reflect the genetic background (ARP1; $p53^{-/-}$ vs H929; $p53^{+/+}$) and RNA changes, as more DNA replication and repair pathways were enriched in ARP1 cell (Figure 6D). However, the most enriched pathway was that of RNA polymerase, which may, therefore, contribute to the enhanced transcripts of TGF-β1 requiring translation. Further studies assessing the therapeutic effects and detailed molecular mechanisms of the bioactive compounds from *Abelmoschus manihot* L. on MM are required.

Conclusion

The current study demonstrated that the bio-active components of HKC significantly influenced cell–cell interaction, cell growth and MM progressing. These results indicated that HKC may serve as a promising anti-MM drug, which has been validated in MM models. However, further studies are necessary to determine the protective mechanism utilized by each bio-active extract on MM cells and the cell microenvironment for MM therapy.

Acknowledgment

This work was supported by National Natural Science Foundation of China 81970196, 81670200 (to CG&YY); Innovation Team of Six Talent Peaks Project in Jiangsu Province (TD-SWYY-015); National Key Research and Development Program-Precision Medicine Sub-program 2016YFC0905900 (to YY); A Project Funded by the Priority Academic Program Development of Jiangsu Higher Education Institutions (Integration of Chinese and Western Medicine).

Disclosure

The authors declare that they have no known competing financial interests or personal relationships that could have appeared to influence the work reported in this paper.

References

1. Rajkumar SV. Myeloma today: disease definitions and treatment advances. *Am J Hematol*. 2016;91(1):90–100. doi:10.1002/ajh.24236
2. Ferlay J, Soerjomataram I, Dikshit R, et al. Cancer incidence and mortality worldwide: sources, methods and major patterns in GLOBOCAN 2012. *Int J Cancer*. 2015;136(5):E359–E386. doi:10.1002/ijc.29210
3. Kawano Y, Moschetta M, Manier S, et al. Targeting the bone marrow microenvironment in multiple myeloma. *Immunol Rev*. 2015;263 (1):160–172. doi:10.1111/imr.12233
4. Manier S, Sacco A, Leleu X, Ghobrial IM, Roccaro AM. Bone marrow microenvironment in multiple myeloma progression. *J Biomed Biotechnol*. 2012;2012:157496. doi:10.1155/2012/157496
5. Chen P, Wan Y, Wang C, et al. [Mechanisms and effects of Abelmoschus manihot preparations in treating chronic kidney disease]. *Zhongguo Zhong Yao Za Zhi*. 2012;37(15):2252–2256.
6. Ge J, Miao JJ, Sun XY, Yu JY. Huangkui capsule, an extract from Abelmoschus manihot (L.) medic, improves diabetic nephropathy via activating peroxisome proliferator-activated receptor (PPAR)-alpha/gamma and attenuating endoplasmic reticulum stress in rats. *J Ethnopharmacol*. 2016;189:238–249. doi:10.1016/j.jep.2016.05.033
7. Zhang L, Li P, Xing CY, et al. Efficacy and safety of Abelmoschus manihot for primary glomerular disease: a prospective, multicenter randomized controlled clinical trial. *Am J Kidney Dis*. 2014;64 (1):57–65. doi:10.1053/j.ajkd.2014.01.431
8. Xue C, Guo J, Qian D, et al. Identification of the potential active components of Abelmoschus manihot in rat blood and kidney tissue by microdialysis combined with ultra-performance liquid chromatography/quadrupole time-of-flight mass spectrometry. *J Chromatogr B Anal Technol Biomed Life Sci*. 2011;879(5–6):317–325. doi:10.1016/j.jchromb.2010.12.016
9. Tu Y, Sun W, Wan YG, et al. Huangkui capsule, an extract from Abelmoschus manihot (L.) medic, ameliorates adriamycin-induced renal inflammation and glomerular injury via inhibiting p38MAPK signaling pathway activity in rats. *J Ethnopharmacol*. 2013;147 (2):311–320. doi:10.1016/j.jep.2013.03.006
10. Wang X-R, Wang Z-Q, Li Y. Studies on the chemical constituents of Abelmoschus manihot L. medic. *Acta Botanica Sinica*. 1981;23 (3):222–227.
11. Lai XY, Zhao YY, Liang H. [Studies on chemical constituents in flower of Abelmoschus manihot]. *Zhongguo Zhong Yao Za Zhi*. 2006;31(19):1597–1600.
12. Lai X, Liang H, Zhao Y, Wang B. Simultaneous determination of seven active flavonols in the flowers of Abelmoschus manihot by HPLC. *J Chromatogr Sci*. 2009;47(3):206–210. doi:10.1093/chromsci/47.3.206
13. Guo J, Shang EX, Duan JA, Tang Y, Qian D, Su S. Fast and automated characterization of major constituents in rat biofluid after oral administration of Abelmoschus manihot extract using ultra-performance liquid chromatography/quadrupole time-of-flight mass spectrometry and metaboLynx. *Rapid Commun Mass Spectrom*. 2010;24(4):443–453. doi:10.1002/rcm.4416
14. Chen Y, Cai G, Sun X, Chen X. Treatment of chronic kidney disease using a traditional Chinese medicine, Flos Abelmoschus manihot (Linnaeus) Medicus (Malvaceae). *Clin Exp Pharmacol Physiol*. 2016;43(2):145–148. doi:10.1111/cep.2016.43.issue-2
15. Ai G, Liu Q, Hua W, Huang Z, Wang D. Hepatoprotective evaluation of the total flavonoids extracted from flowers of Abelmoschus manihot (L.) Medic: in vitro and in vivo studies. *J Ethnopharmacol*. 2013;146(3):794–802. doi:10.1016/j.jep.2013.02.005
16. Wu LL, Yang XB, Huang ZM, Liu HZ, Wu GX. In vivo and in vitro antiviral activity of hyperoside extracted from Abelmoschus manihot (L) medik. *Acta Pharmacol Sin*. 2007;28(3):404–409. doi:10.1111/j.1745-7254.2007.00510.x
17. Yang S-Y, Zhao Y-M, Li Z-L, Zuo Q-Y, Qian S-H. Flavonoids from flowers of Abelmoschus manihot. *Chem Nat Compound*. 2018;54 (2):257–260. doi:10.1007/s10600-018-2317-z
18. Livak KJ, Schmittgen TD. Analysis of relative gene expression data using real-time quantitative PCR and the 2(-Delta Delta C(T)) method. *Methods*. 2001;25(4):402–408. doi:10.1006/meth.2001.1262
19. Schmittgen TD, Livak KJ. Analyzing real-time PCR data by the comparative C(T) method. *Nat Protoc*. 2008;3(6):1101–1108. doi:10.1038/nprot.2008.73
20. Yuan X, Li T, Xiao E-L, et al. Licochalcone B inhibits growth of bladder cancer cells by arresting cell cycle progression and inducing apoptosis. *Food Chem Toxicol*. 2014;65:242–251. doi:10.1016/j.fct.2013.12.030
21. Sun S-Y, Du G-Y, Xue J, et al. PCC0208009 enhances the anti-tumor effects of temozolomide through direct inhibition and transcriptional regulation of indoleamine 2,3-dioxygenase in glioma models. *Int J Immunopathol Pharmacol*. 2018;(2018:32.
22. Kang H, Jha S, Deng Z, et al. Somatic activating mutations in MAP2K1 cause melorheostosis. *Nat Commun*. 2018;9(1):1390. doi:10.1038/s41467-018-03720-z
23. Lai X, Zhao Y, Liang H, Bai Y, Wang B, Guo D. SPE-HPLC method for the determination of four flavonols in rat plasma and urine after oral administration of Abelmoschus manihot extract. *J Chromatogr B Anal Technol Biomed Life Sci*. 2007;852(1–2):108–114. doi:10.1016/j.jchromb.2006.12.043
24. Stambolic V, Ruel L, Woodgett JR. Lithium inhibits glycogen synthase kinase-3 activity and mimics wingless signalling in intact cells. *Curr Biol*. 1996;6(12):1664–1668. doi:10.1016/S0960-9822(02)70790-2
25. Guo J, Du L, Shang E, et al. Conjugated metabolites represent the major circulating forms of Abelmoschus manihot in vivo and show an altered pharmacokinetic profile in renal pathology. *Pharm Biol*. 2016;54(4):595–603. doi:10.3109/13880209.2015.1068337
26. Derksen PW, Tjin E, Meijer HP, et al. Illegitimate WNT signaling promotes proliferation of multiple myeloma cells. *Proc Natl Acad Sci USA*. 2004;101(16):6122–6127. doi:10.1073/pnas.0305855101
27. Qiang YW, Chen Y, Brown N, et al. Characterization of Wnt/beta--catenin signalling in osteoclasts in multiple myeloma. *Br J Haematol*. 2010;148(5):726–738. doi:10.1111/j.1365-2141.2009.08009.x
28. Houben A, Kostanova-Poliakova D, Weissenbock M, et al. Beta-catenin activity in late hypertrophic chondrocytes locally orchestrates osteoblastogenesis and osteoclastogenesis. *Development*. 2016;143 (20):3826–3838. doi:10.1242/dev.137489
29. van Andel H, Kocemba KA, Spaargaren M, Pals ST. Aberrant Wnt signaling in multiple myeloma: molecular mechanisms and targeting options. *Leukemia*. 2019;33(5):1063–1075. doi:10.1038/s41375-019-0404-1

30. Yao R, Sun X, Xie Y, et al. Lithium chloride inhibits cell survival, overcomes drug resistance, and triggers apoptosis in multiple myeloma via activation of the Wnt/beta-catenin pathway. *Am J Transl Res*. 2018;10(8):2610–2618.
31. Sukhdeo K, Mani M, Hideshima T, et al. beta-catenin is dynamically stored and cleared in multiple myeloma by the proteasome-aggresome-autophagosome-lysosome pathway. *Leukemia*. 2012;26(5):1116–1119. doi:10.1038/leu.2011.303
32. Kawano M, Hirano T, Matsuda T, et al. Autocrine generation and requirement of BSF-2/IL-6 for human multiple myelomas. *Nature*. 1988;332(6159):83–85. doi:10.1038/332083a0
33. Matthes T, Manfroi B, Zeller A, Dunand-Sauthier I, Bogen B, Huard B. Autocrine amplification of immature myeloid cells by IL-6 in multiple myeloma-infiltrated bone marrow. *Leukemia*. 2015;29(9):1882–1890. doi:10.1038/leu.2015.145
34. Rosean TR, Tompkins VS, Olivier AK, et al. The tumor microenvironment is the main source of IL-6 for plasma cell tumor development in mice. *Leukemia*. 2015;29(1):233–237. doi:10.1038/leu.2014.260
35. Ribatti D, Nico B, Vacca A. Importance of the bone marrow microenvironment in inducing the angiogenic response in multiple myeloma. *Oncogene*. 2006;25(31):4257–4266. doi:10.1038/sj.onc.1209456
36. Hideshima T, Chauhan D, Schlossman R, Richardson P, Anderson KC. The role of tumor necrosis factor alpha in the pathophysiology of human multiple myeloma: therapeutic applications. *Oncogene*. 2001;20(33):4519–4527. doi:10.1038/sj.onc.1204623
37. Urashima M, Chen BP, Chen S, et al. The development of a model for the homing of multiple myeloma cells to human bone marrow. *Blood*. 1997;90(2):754–765. doi:10.1182/blood.V90.2.754
38. Dankbar B, Padro T, Leo R, et al. Vascular endothelial growth factor and interleukin-6 in paracrine tumor-stromal cell interactions in multiple myeloma. *Blood*. 2000;95(8):2630–2636. doi:10.1182/blood.V95.8.2630
39. Massague J. TGFbeta in Cancer. *Cell*. 2008;134(2):215–230. doi:10.1016/j.cell.2008.07.001